# Thermal Switching of the Reflection in Chiral Nematic Mesoporous Organosilica Films Infiltrated with Liquid Crystals

8 AUTHORS, INCLUDING:

Michael Giese (nee Müller)
University of Duisburg-Essen
36 PUBLICATIONS   363 CITATIONS

SEE PROFILE

Ronald Y Dong
University of British Columbia - Vancouver
220 PUBLICATIONS   2,270 CITATIONS

SEE PROFILE

Carl A Michal
University of British Columbia - Vancouver
49 PUBLICATIONS   1,583 CITATIONS

SEE PROFILE

Mark J MacLachlan
University of British Columbia - Vancouver
166 PUBLICATIONS   5,267 CITATIONS

SEE PROFILE

# Thermal Switching of the Reflection in Chiral Nematic Mesoporous Organosilica Films Infiltrated with Liquid Crystals

Michael Giese,[†] Joanna C. De Witt,[†] Kevin E. Shopsowitz,[†] Alan P. Manning,[‡] Ronald Y. Dong,[‡] Carl A. Michal,[‡] Wadood Y. Hamad,[§] and Mark J. MacLachlan*,[†]

[†]Department of Chemistry, University of British Columbia, 2036 Main Mall, Vancouver, British Columbia V6T 1Z1, Canada

[‡]Department of Physics and Astronomy, University of British Columbia, 6224 Agricultural Road, Vancouver, British Columbia V6T 1Z1, Canada

[§]FPInnovations, 3800 Wesbrook Mall, Vancouver, British Columbia V6S 2L9, Canada

Ⓢ Supporting Information

**ABSTRACT:** Materials that undergo stimulus-induced optical changes are important for many new technologies. In this paper, we describe a new free-standing silica-based composite film that exhibits reversible thermochromic reflection, induced by a liquid crystalline guest in the pores of iridescent mesoporous films. We demonstrate that selective reflection from the novel mesoporous organosilica material with chiral nematic organization can be reversibly switched by thermal cycling of the 8CB guest between its isotropic and liquid crystalline states, which was proven by solid-state NMR experiments. The switching of the optical properties of the chiral solid-state host by stimulus-induced transitions of the guest opens the possibility of applications for these novel materials in sensors and displays.



**KEYWORDS:** chiral nematic, mesoporous silica, 8CB, liquid crystal, thermal switching
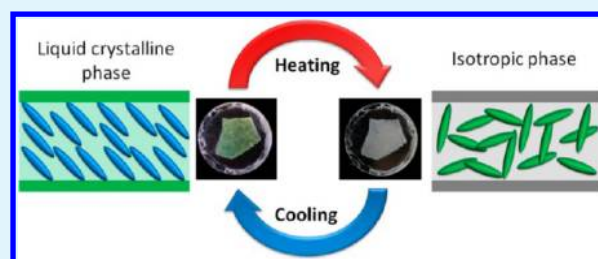
## INTRODUCTION

The ability to reversibly control the optical properties of photonic crystals is attractive for many applications including reflective displays and sensors.[1−8] Band structures of photonic crystals depend on both their periodicity and the refractive index contrast between their constituent dielectric materials; it is therefore possible to modulate the optical properties of photonic crystals by addressing either of these structural parameters. The refractive index contrast of porous photonic crystals (e.g., inverse opals) is readily varied by infiltrating the pores with different substances, such as vapors and liquids.[9−15] Further control over the optical properties of porous photonic crystals can be achieved through loading the pores with stimuli-responsive materials. Liquid crystals (LCs), which can show large changes in orientation and refractive index in response to different stimuli, have been studied in this regard.[16,17] A number of photonic crystals infiltrated with LCs are known and show interesting properties upon phase transition of the mesogens inside the periodic structure.[18−22] Neubert et al. prepared photonic crystals infiltrated with 4-cyano-4′-pentylbiphenyl (5CB) showing polarization-dependent optical properties due to the orientation of the LC in its liquid crystalline phase.[23] Another study reports on a similar effect in indium phosphide-based planar photonic crystals infiltrated with a nematic liquid crystal.[24] Recently, Lemieux, Crudden et al. reported on mesoporous organosilicas with axially chiral biphenyl groups transferring the chirality to bulk liquid crystals.[25] However, the influence of the liquid crystal on the mesoporous host materials was not explored.

Chiral nematic liquid crystals (CNLCs) consist of mesogens arranged in a periodic helical structure and can be considered as a type of 1D photonic crystal.[26] In the case of thermotropic CNLCs, the repeating distance (i.e., $P$, the pitch, or $P/2$ in the case of symmetrical mesogens) is typically sensitive to temperature, pressure, and the presence of external fields, making these materials useful for applications such as color changing thermometers and reflective displays.[27−29] The formation of a chiral nematic phase usually requires the presence of molecular chirality; Brett and co-workers, however, demonstrated an alternative approach to inducing a chiral nematic phase by introducing an achiral liquid crystal into a thin film of inorganic helical micropillars formed through the glancing-angle deposition (GLAD) technique.[30−33] An advantage of this approach is that the high surface area of GLAD films allows for a greater level of control over LC alignment than can be achieved by surface treatment alone. Additionally, the switching of LCs embedded in GLAD films with applied fields remains possible and can be used to modify their optical properties.[34−36]
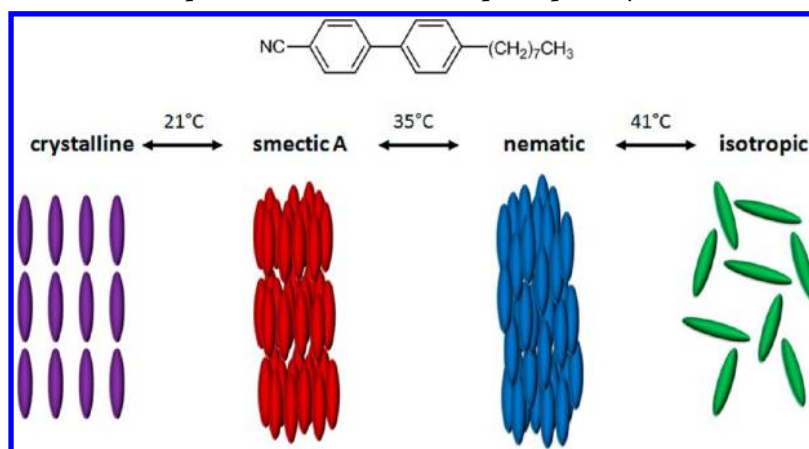
We recently reported convenient methods to make high surface area chiral nematic mesoporous silica (CNMS),[37]

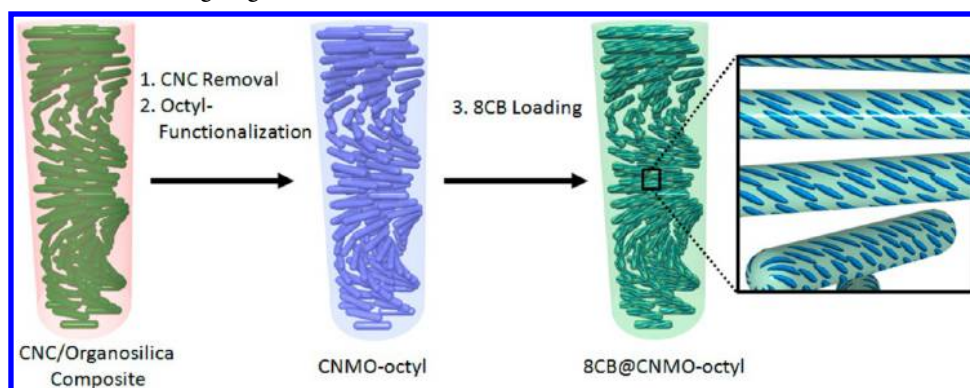**Scheme 1. Structure and Transition Temperatures of the Thermotropic Liquid-Crystalline 8CB**



**Scheme 2. Synthesis and Functionalization of the Chiral Nematic Mesoporous Organosilica Composites, and Subsequent Loading of the Films with 8CB Aligning in the Pores**



organosilica (CNMO),[38] or carbon films (CNMC)[39] by using cellulose nanocrystals (CNCs) as a chiral nematic template.[40−54] The CNMS and CNMO materials behave as porous 1D photonic crystals that selectively reflect circularly polarized light in an analogous way to CNLCs and appear iridescent when their helical pitch is on the length scale of ∼350−500 nm. As with other porous photonic crystals, infiltrating the pores of CNMS and CNMO films with different materials causes a large change in their optical properties. For example, we have previously shown that loading these films with isotropic liquids essentially shuts off their photonic properties because of near refractive index matching.[37,38]

The present study reports the reversible modification of the photonic properties of CNMO films by infiltrating their mesopores with a thermally responsive guest. 4-Cyano-4′-octylbiphenyl (8CB), a thermotropic liquid crystal (Scheme 1),[55] was identified as an excellent candidate because it is commercially available and it shows significant differences in the refractive index (1.51−1.68) depending on the liquid crystalline phase and orientation of the optical axis.[56] Because the peak wavelength ($\lambda_{max}$) of the reflected light normal to the surface of the chiral nematic host is related to the average refractive index ($n_{avg}$), and helical pitch of the structure ($P$), the color of the chiral nematic composite can be varied by changing the refractive index of a guest inside the pores of the chiral nematic mesoporous material according to the following equation:[57]

$$\lambda_{max} = n_{avg}P$$

Here we describe the synthesis of octyl-functionalized chiral nematic mesoporous organosilica, its infiltration with 8CB, and subsequent investigations of these new composite materials with respect to their reversibly switchable optical properties. The composites are iridescent, show a peak reflected wavelength in the visible range, and undergo a reversible transition at around 40 °C; above this temperature, colorless, transparent films are obtained. This unique switching of a guest within the pores of the chiral nematic solid-state host may serve as the basis of a tunable filter or display. To understand the behavior of the composite films on a molecular level, we synthesized $^{15}$N-labeled 8CB ($^{15}$N-8CB) and studied its alignment within the pores of the mesoporous host by solid-state NMR spectroscopy.

## ■ RESULTS AND DISCUSSION

Ethylene-bridged chiral nematic mesoporous organosilica (CNMO) films used in this study as host for the liquid crystal were synthesized according to a previously reported procedure.[37,38] Briefly, a homogeneous mixture of 1,2-bis-(trimethoxysilyl)ethane (BTMSE) and CNCs was slowly dried to give free-standing composite films. The CNC template was removed by acid hydrolysis in $H_2SO_4$(aq) followed by an oxidative treatment in $H_2O_2/H_2SO_4$(aq) to remove insoluble cellulosic byproducts (Scheme 2). The organosilica films retained a chiral nematic pore structure as evidenced by a strong reflection peak at 420 nm (Figure 1a) and scanning electron microscopy (Figure 1b), which shows the typical layered structure of these materials.
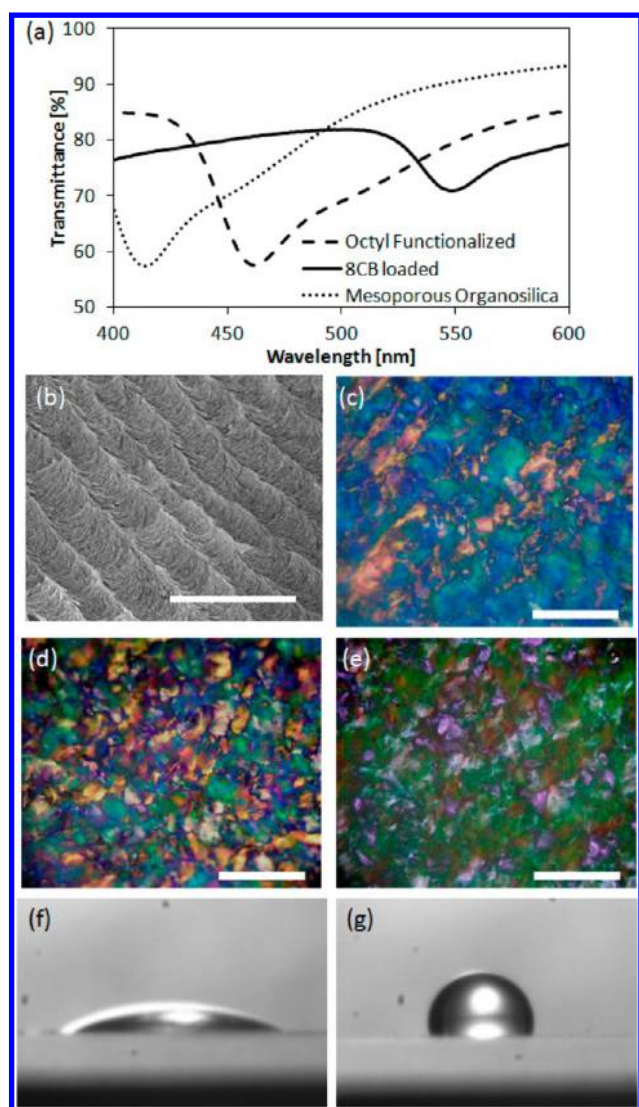
**Figure 1.** Characterization of the organosilica films and composites. (a) UV−vis spectra of the mesoporous organosilica film, the octyl-functionalized organosilica film, and the octyl-functionalized organosilica film loaded with 8CB. (b) SEM image of the host material showing the characteristic left-handed twist of the layers (scale bar, 2 μm). (c−e) POM images of the mesoporous organosilica film, the octyl-functionalized organosilica film, and the 8CB loaded octyl-functionalized organosilica film, respectively, viewed under crossed polarizers (scale bar, 300 μm). Contact angle images of a drop of water on (f) the mesoporous organosilica and (g) the octyl-functionalized organosilica.

Initially, 8CB@CNMO composites were investigated with respect to their optical behavior upon heating. However, although the samples show a reversible change in color upon heating the composites to 40−50 °C, they showed a broad transition. Therefore, the pores of the CNMO were functionalized with *n*-octyl (CNMO-octyl) to improve the compatibility of the CNMO host and the liquid crystalline guest. The preparation of the 8CB@CNMO-octyl composites is shown in Scheme 2.

The CNMO and the novel octyl-functionalized material were characterized by elemental analysis, contact angle measurements, thermogravimetric analysis (TGA), gas adsorption, polarized optical microscopy (POM) and UV−vis, IR and circular dichroism (CD) spectroscopies. The POM images for the as synthesized organosilica and the *n*-octyl functionalized films show a characteristic birefringence under crossed polarizers (Figure 1c, d). Elemental analysis, TGA (see Figure S1 in the Supporting Information), IR spectroscopy (see Figure S2 in the Supporting Information), and contact angle measurements give evidence for the successful functionalization of the CNMO films. The functionalization was quantified by elemental analysis,[58] showing a ratio of ∼1:10 of the octyl groups to ethylene bridges, which is in agreement with the TGA data. Although the pores of the as-synthesized CNMO samples are hydrophilic and readily absorb water (initial contact angle of 28°, Figure 1f), the CNMO-octyl films are hydrophobic and show an initial contact angle of 98° with only slight changes after several minutes (decreasing by 0−2%, Figure 1g). However, to prove that the octyl functionalization occurs in the pores rather than exclusively on the surface of the CNMO films, we undertook $N_2$ adsorption measurements on CNMO and CNMO-octyl films. Both samples reveal type IV adsorption isotherms with type H2 hysteresis loops (see Figure S3 in the Supporting Information) with Brunauer−Emmett−Teller (BET) surface areas of 555 and 416 $m^2$ $g^{-1}$ and pore volumes of 1.3 and 0.96 $cm^3$ $g^{-1}$ for CNMO and CNMO-octyl, respectively. In addition, the films show fairly uniform Barrett, Joyner, and Halenda (BJH) peak pore diameters of 7.1 (CNMO) and 4.7 nm (CNMO-octyl). The decrease in the surface area, pore volume, and pore diameter of the CNMO-octyl films compared to the CNMO samples is consistent with functionalizing the interior surface of the mesoporous organosilica with octylsilyl groups. Further evidence for the functionalization of the pores is provided by UV−vis spectra (Figure 1a), which show the reflection peak originating from chiral nematic order in the films. The absorption maximum of CNMO redshifts slightly from 420 to 460 nm for CNMO-octyl, which is consistent with a change of the average refractive index of the mesoporous films upon functionalization.

To obtain the 8CB@CNMO-octyl composite, the liquid-crystalline 8CB was heated to 50 °C (isotropic phase) and injected using a micropipet (see Scheme 2). Immediately after infiltration of the pores with isotropic 8CB, the initially green films become clear and colorless. The color returns upon cooling the sample to room temperature and POM images show the characteristic texture of the host material (Figure 1e). The composite films were characterized by IR and UV−vis spectroscopy as well as by POM, elemental analysis, TGA, and X-ray diffraction (XRD). IR spectroscopy of the films showed signals at 2230 (CN stretching), 1600 and 1500 $cm^{-1}$ (see Figure S2d in the Supporting Information) that are diagnostic of 8CB. Elemental analysis (37 wt %)[59] and TGA (30 wt %, see Figure S1d in the Supporting Information) both showed that the samples contained ca. 35 wt % 8CB loaded into the pores, equating to a ∼55% pore filling with 8CB.[60] Further evidence that the 8CB infiltrates the mesopores comes from UV−vis spectroscopy, where a significant red shift of the reflectance peak of the films from 460 to ∼550 nm occurs, causing the films to appear green in color (Figures 1a and 2a).

As already mentioned in the Introduction, our aim is to study the thermochromic behavior of the new 8CB@CNMO-octyl composite. POM images of 8CB@CNMO-octyl at room temperature show birefringence and a texture similar to the pristine chiral nematic silica and organosilica films (Figure 2b).[37,38] However, upon heating, the birefringence of composite films disappears (Figure 2c). The complete loss of birefringence at 48 °C is indicative of the phase transition of the
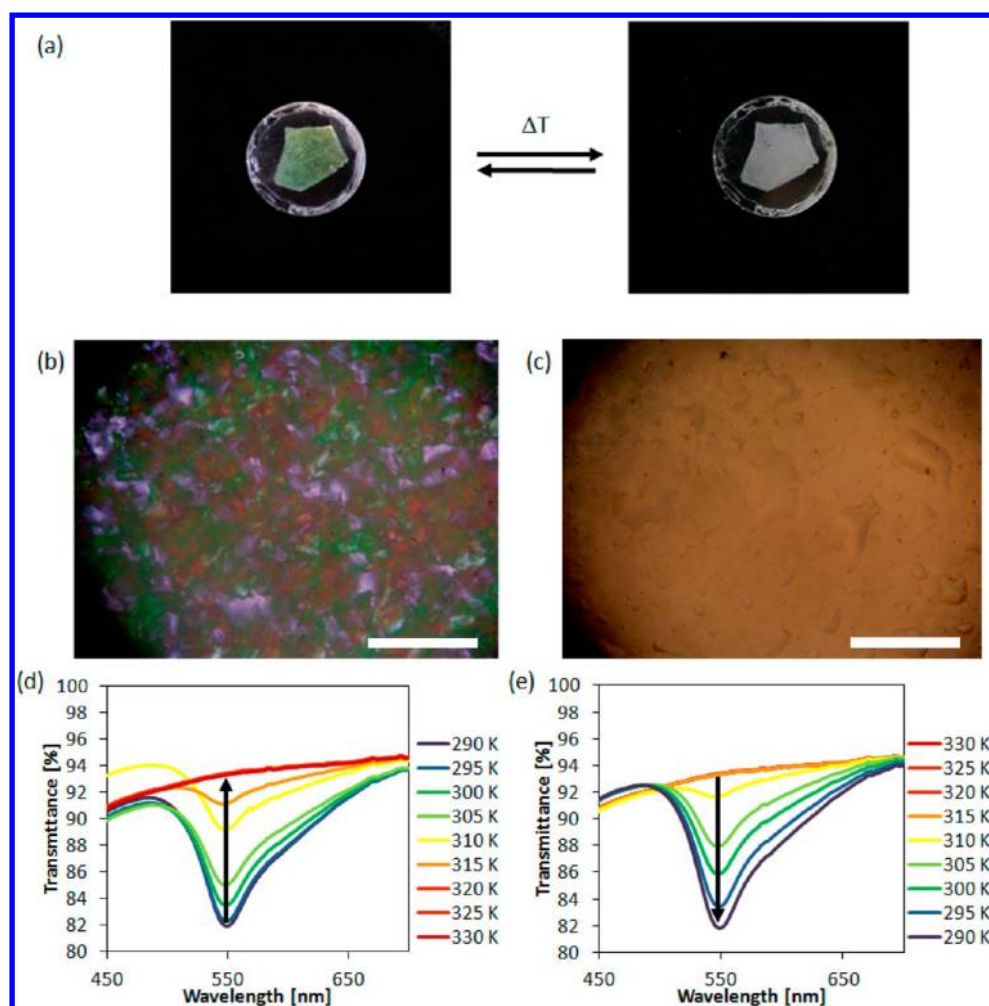
**Figure 2.** (a) Thermochromic behavior of the novel 8CB@CNMO-octyl composite showing the color change from green to colorless upon heating to 48 °C. (b, c) Variable-temperature POM images of 8CB loaded octyl-functionalized organosilica films at (b) 21 and (c) 48 °C show the complete loss of color and birefringence upon heating. The micrographs were taken with crossed polarizers (scale bar, 300 $\mu$m). (d, e) Normalized variable-temperature UV−vis spectra of 8CB@CNMO upon (d) heating and (e) cooling demonstrate the reversible loss of structural color upon heating by following the peak at 550 nm.

liquid crystalline 8CB to the isotropic state. Because the refractive index of the isotropic liquid inside the pores nearly matches the refractive index of the host material, both the birefringence and the color of the 8CB@CNMO-octyl are suppressed.

We undertook a variable-temperature UV−vis spectroscopy study of the 8CB-loaded films to quantify the change in color upon heating from room temperature to 60 °C. A large increase in the transmittance of the signal appearing at 550 nm in the UV−vis spectrum was observed for temperatures between 37 and 42 °C with complete extinction of the signal at 47 °C (Figure 2d). Subsequent cooling of the sample in 5 °C steps shows the reversible nature of the transition with a slight hysteresis that might be attributed to the confinement of the mesogens inside the mesopores(Figure 2e).[61] Although 8CB is known to have two different liquid-crystalline phases (smectic and nematic), only the transition from the nematic to the isotropic state seems to affect the color of the composite material. Confinement and surface effects have been shown previously to result in significant shifting and broadening of the transition temperatures of nCB liquid crystals.[62,63] Furthermore, it was shown that the confinement effect is even stronger for the smectic phase.[64,65] Therefore, it is likely that the chiral

nematic order of tje host material and the interaction with the octyl groups on the surface suppresses a smectic organization of the 8CB inside the pores.

To get a deeper understanding of the alignment of the mesogen molecules inside the mesoporous films, we performed XRD and solid-state NMR measurements of the composites. The XRD data collected at room temperature show only a broad halo that is indicative of the presence of liquid crystalline 8CB inside the pores of the composite (see Figure S4 in the Supporting Information). However, it gives no information on the alignment of the mesogens with respect to the pores of 8CB@CNMO-octyl. To further probe the alignment, we synthesized the $^{15}$N labeled analogue of 8CB ($^{15}$N-8CB), injected it into the pores of the CNMO, and performed angle-dependent $^{15}$N solid-state NMR experiments of the loaded films. The wide-line $^{15}$N NMR spectra of the $^{15}$N-8CB-loaded films collected at 21 °C (Figure 3) clearly demonstrate alignment of the 8CB mesogens within the porous structure, as the NMR line shape shows a dramatic dependence on the orientation of the films in the magnetic field. The breadth of the spectra arises from the large chemical shift anisotropy of the cyano headgroup (typically ~390 ppm for para-substituted benzonitriles).[66] With $\theta$ defined as the angle between the film
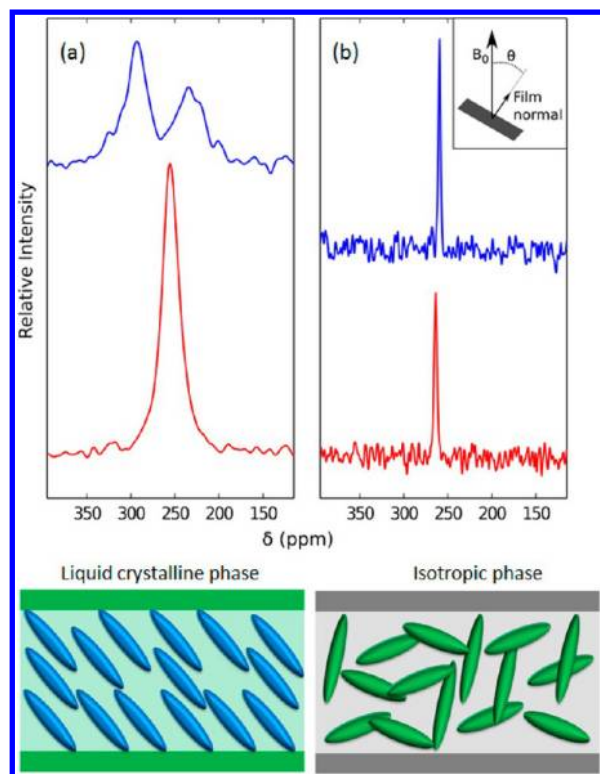
**Figure 3.** ^{15}N wide-line NMR spectra of [15]N-8CB-loaded films (top) as well as a schematic representation of the alignment of the mesogens in the pores at (a) 21 and (b) 60 °C. The upper curves (in blue) were collected with $\theta = 90°$, whereas for the lower curves (red) $\theta = 0°$. The inset shows the definition of $\theta$ as the angle between the film normal and the $B_0$ field.

normal and the $B_0$ field, when $\theta = 90°$ the spectrum is approximately a two-dimensional (2D) planar powder pattern,[67] with an intense perpendicular edge at 300 ppm and a less intense parallel edge at 230 ppm. This asymmetry in edge intensity suggests that the mesogens may not form a perfect planar distribution with respect to the film normal. In addition, the width of the 2D powder pattern is considerably less than the 390 ppm expected for a static distribution, indicating the presence of some motional (e.g., rotation- and translation-diffusion) averaging. When $\theta = 0°$, the broad pattern collapses to a sharper single peak. Together these spectra suggest that the distribution of orientations of the 8CB molecules have nearly cylindrical symmetry about the film normal, which is consistent with the helical structure present in the host. A simple model of a planar distribution of averaged chemical shift anisotropy (CSA) tensors would predict that the single peak in the $\theta = 0°$ spectrum would lie at the position of the perpendicular edge of the $\theta = 90°$ spectrum. The fact it does not lie there implies deviation from a planar distribution, possibly because of the chiral nematic organization of the host or competition between magnetic field-induced alignment and surface-induced alignment.

When the sample was heated to the isotropic phase, the spectra collapse to a very sharp, liquidlike peak, shown in Figure 3b. The position of the spectral peak does show some dependence on the film orientation, likely due to susceptibility effects of the film stack, not from any residual alignment. The shift is seen to approximately follow the $\sin^2(\theta)$ dependence expected for stacks of alternating susceptibility,[68] where $\theta$ has been defined above. It is noted that the lower temperature of 21 °C is exactly the bulk crystallization temperature of 8CB. However, the spectrum gradually broadens but does not change abruptly as the temperature is lowered from 30 to 0 °C, indicating that crystallization is suppressed. This is similar to the behavior of confined liquid crystals in other porous systems such as Vycor and aerogel.[69,70]

## CONCLUSION

We have demonstrated for the first time that hydrophobic octyl-functionalized CNMO is an excellent host for the liquid crystal 8CB. Variable-temperature UV−vis and POM studies showed that the 8CB/organosilica composite undergoes a reversible thermochromic switching at a temperature that correlates well with the transition of the liquid crystalline to the isotropic phase of bulk 8CB. Solid-state NMR experiments of ^{15}N-labeled 8CB correlate the change in the optical appearance of the material to a switch in the molecular order of the mesogens inside the pores. Our approach of stimulus-induced switching of a guest to modify the optical properties of a mesoporous host may lead to the development of dynamically switchable devices in displays or sensors. Detailed studies on other nematic liquid crystals, which will allow for the thermal response of the CNMO films to be readily tuned, as well as detailed solid-state NMR and modeling studies are underway and will be reported in due course.

## ASSOCIATED CONTENT

**S** **Supporting Information**
Experimental procedures, thermogravimetric analysis data, IR spectra, gas adsorption data, and X-ray diffraction data. This material is available free of charge via the Internet at http://pubs.acs.org.

## AUTHOR INFORMATION

**Corresponding Author**
*E-mail: mmaclach@chem.ubc.ca. Fax: (+1) 604-822-2847.

**Author Contributions**
M.G. and J.C.D.W. contributed equally to this work.

**Notes**
The authors declare no competing financial interest.

## ACKNOWLEDGMENTS

## REFERENCES

(1) Aguirre, C. I.; Reguera, E.; Stein, A. *Adv. Funct. Mater.* **2010**, *20*, 2565−2578.
(2) Zhao, Y.; Xie, Z.; Gu, H.; Zhu, C.; Gu, Z. *Chem. Soc. Rev.* **2012**, *41*, 3297−3317.
(3) Lee, K.; Asher, S. A. *J. Am. Chem. Soc.* **2000**, *122*, 9534−9537.
(4) Link, J. R.; Sailor, M. J. *Proc. Natl. Acad. Sci. U.S.A.* **2003**, *100*, 10607−10610.
(5) Ruminski, A. M.; Barillaro, G.; Chaffin, C.; Sailor, M. J. *Adv. Funct. Mater.* **2011**, *21*, 1511−1525.
(6) King, B. H.; Wong, T.; Sailor, M. J. *Langmuir* **2011**, *27*, 8576−8585.
(7) Bonifacio, L. D.; Puzzo, D. P.; Breslav, S.; Willey, B. M.; McGeer, A.; Ozin, G. A. *Adv. Mater.* **2010**, *22*, 1351−1354.

6858

dx.doi.org/10.1021/am402266z | *ACS Appl. Mater. Interfaces* 2013, 5, 6854−6859

(8) Peng, H.; Wang, S.; Zhang, Z.; Xiong, H.; Li, J.; Chen, L.; Li, Y. *J. Agric. Food Chem.* **2012**, *60*, 1921−1928.

(9) Schroden, R. C.; Al-Daous, M.; Blanford, C. F.; Stein, A. *Chem. Mater.* **2002**, *14*, 3305−3315.

(10) Li, Y. Y.; Cunin, F.; Link, J. R.; Gao, T.; Betts, R. E.; Reiver, S. H.; Chin, V.; Bhatia, S. N.; Sailor, M. J. *Science* **2003**, *229*, 2045−2047.

(11) Potyrailo, R. A.; Ghiradella, H.; Vertiatchikh, A.; Dovidenko, K.; Cournoyer, J. R.; Olson, E. *Nat. Photon.* **2007**, *1*, 123−128.

(12) Colodrero, S.; Ocana, M.; Gonzalez-Elipe, A. R.; Miguez, H. *Langmuir* **2008**, *24*, 9135−9139.

(13) Kobler, J.; Lotsch, B. V.; Ozin, G. A.; Bein, T. *ACS Nano* **2009**, *3*, 1669−1676.

(14) Burgess, I. B.; Mishchenko, L.; Hatton, B. D.; Kolle, M.; Loncar, M.; Aizenberg, J. *J. Am. Chem. Soc.* **2011**, *133*, 12430−12432.

(15) Liu, C.; Gao, G.; Zhang, Y.; Wang, L.; Wang, J.; Song, Y. *Macromol. Rapid Commun.* **2012**, *33*, 380−385.

(16) Kitzerow, H.-S.; Lorenz, A.; Matthias, H. In *Nanophotonic Materials* Wehrspohn, R. B., Kitzerow, H.-S., Busch, K., Eds.; Wiley-VCH: Weinheim, Germany, 2008, pp 221−238.

(17) Kitzerow, H.-S.; Lorenz, A.; Matthias, H. *Phys. Status Solidi (a)* **2007**, *204*, 3754−3767.

(18) Mertens, G.; Wehrspohn, R. B.; Kitzerow, H.-S.; Matthias, S.; Jamois, C.; Gösele, U. *Appl. Phys. Lett.* **2005**, *87*, 241108.

(19) Ghattan, Z.; Hasek, T.; Wilk, R.; Shahabadi, M.; Koch, M. *Opt. Commun.* **2008**, *281*, 4623−4625.

(20) Kubo, S.; Gu, Z.-Z.; Takahashi, K.; Fujishima, A.; Segawa, H.; Sato, O. *J. Am. Chem. Soc.* **2004**, *126*, 8314−8319.

(21) Kubo, S.; Gu, Z.-Z.; Takahashi, K.; Fujishima, A.; Segawa, H.; Sato, O. *Chem. Mater.* **2005**, *17*, 2298−2309.

(22) Liu, Y. J.; Cai, Z.; Leong, E. S. P.; Zhao, X. S.; Teng, J. H. *J. Mater. Chem.* **2012**, *22*, 7609−7613.

(23) Mertens, G.; Röder, T.; Matthias, H.; Marsmann, H.; Kitzerow, H.-S. R.; Schweizer, S. L.; Jamois, C.; Wehrspohn, R. B.; Neubert, M. *Appl. Phys. Lett.* **2003**, *83*, 3036−3038.

(24) Martz, J.; Ferrini, R.; Nüesch, F.; Zuppiroli, L.; Wild, B.; Dunbar, L. A.; Houdré, R.; Mulot, M.; Anand, S. *J. Appl. Phys.* **2006**, *99*, 103105.

(25) Jayalakshmi, V.; Wood, T.; Basu, R.; Du, J.; Blackburn, T.; Rosenblatt, C.; Crudden, C. M.; Lemieux, R. P. *J. Mater. Chem.* **2012**, *22*, 15255−15261.

(26) Reinitzer, F. *Monatsh. Chem.* **1888**, *9*, 421−441.

(27) Fergason, J. L. *Appl. Opt.* **1968**, *7*, 1729−1737.

(28) Yang, D. K.; Doane, J. W.; Yaniv, Z.; Glasser, J. *Appl. Phys. Lett.* **1994**, *64*, 1905−1907.

(29) Broer, D. J.; Lub, J.; Mol, G. N. *Nature* **1995**, *378*, 467−469.

(30) Robbie, K.; Brett, M. J. *J. Vac. Sci. Technol. A* **1997**, *15*, 1460−1465.

(31) Kennedy, S. R.; Sit, J. C.; Broer, D. J.; Brett, M. J. *Liq. Cryst.* **2001**, *28*, 1799−1803.

(32) Hodgkinson, I.; Wu, Q. H. *Adv. Mater.* **2001**, *13*, 889−897.

(33) Robbie, K.; Broer, D. J.; Brett, M. J. *Nature* **1999**, *399*, 764−766.

(34) Sit, J. C.; Broer, D. J.; Brett, M. J. *Liq. Cryst.* **2000**, *27*, 387−391.

(35) Wakefield, N. G.; Elias, A. L.; Brett, M. J.; Sit, J. C.; Broer, D. J. *Mol. Cryst. Liq. Cryst.* **2007**, *475*, 85−96.

(36) Sit, J. C.; Broer, D. J.; Brett, M. J. *Adv. Mater.* **2000**, *12*, 371−373.

(37) Shopsowitz, K. E.; Qi, H.; Hamad, W. Y.; MacLachlan, M. J. *Nature* **2010**, *468*, 422−425.

(38) Shopsowitz, K. E.; Hamad, W. Y.; MacLachlan, M. J. *J. Am. Chem. Soc.* **2012**, *134*, 867−870.

(39) Shopsowitz, K. E.; Hamad, W. Y.; MacLachlan, M. J. *Angew. Chem., Int. Ed.* **2011**, *50*, 10991−10995.

(40) Fox, J. D.; Capadona, J. R.; Marasco, P. D.; Rowan, S. J. *J. Am. Chem. Soc.* **2013**, *135*, 5167−5174.

(41) Fernandes, S. N.; Geng, Y.; Vignolini, S.; Glover, B. J.; Trindade, A. C.; Canejo, J. P.; Almeida, P. L.; Brogueira, P.; Godhino, M. H. *Macromol. Chem. Phys.* **2013**, *214*, 25−32.

(42) Zhou, C.; Shi, Q.; Guo, W.; Terrell, L.; Qureshi, A. T.; Hayes, D. J.; Wu, Q. *ACS Appl. Mater. Interfaces* **2013**, *5*, 3847−3854.

(43) Beck, S.; Bouchard, J.; Chauve, G.; Berry, R. *Cellulose* **2013**, *20*, 1401−1411.

(44) Jiang, F.; Hsieh, Y.-L. *Carbohydr. Polym.* **2013**, *95*, 32−40.

(45) Picard, G.; Simon, D.; Kadiri, Y.; LeBreux, J. D.; Ghozayel, F. *Langmuir* **2012**, *28*, 14799−14807.

(46) Salajková, M.; Berglund, L. A.; Zhou, Q. *J. Mater. Chem.* **2012**, *22*, 19798−19805.

(47) Shafiei-Sabet, S.; Hamad, W. Y.; Hatzikiriakos, S. G. *Langmuir* **2012**, *28*, 17124−17133.

(48) Kelly, J. A.; Shopsowitz, K. E.; Ahn, J. M.; Hamad, W. Y.; MacLachlan, M. J. *Langmuir* **2012**, *28*, 17256−17262.

(49) Liu, H.; Shang, S.; Song, Z.; Wang, D. *ACS Appl. Mater. Interfaces* **2012**, *4*, 2413−2419.

(50) Majoinen, J.; Kontturi, E.; Ikkala, O.; Gray, D. G. *Cellulose* **2012**, *19*, 1599−1605.

(51) Hamad, W. Y. *Can. J. Chem. Eng.* **2006**, *84*, 513−519.

(52) Klemm, D.; Kramer, F.; Moritz, S.; Lindström, T.; Ankerfors, M.; Gray, D.; Dorris, A. *Angew. Chem., Int. Ed.* **2011**, *50*, 5438−5466.

(53) Olsson, R. T.; Azizi Samir, M. A. S.; Salazar-Alvarez, G.; Belova, L.; Ström, V.; Berglund, L. A.; Ikkala, O.; Nogués, J.; Gedde, U. W. *Nat. Nanotechnol.* **2010**, *5*, 584−588.

(54) Korhonen, J. T.; Kettunen, M.; Ras, R. H. A.; Ikkala, O. *ACS Appl. Mater. Interfaces* **2011**, *3*, 1813−1816.

(55) Karat, P. P.; Madhusudana, N. V. *Mol. Cryst. Liq. Cryst.* **1976**, *36*, 51−64.

(56) Horn, R. G. *J. Physique* **1978**, *39*, 105−109.

(57) De Vries, H. L. *Acta Crystallogr.* **1951**, *4*, 219−226.

(58) Assuming a fully condensed structure with a formula of $[O_{1.5}SiCH_2CH_2SiO_{1.5}]_{10}[O_{1.5}SiC_8H_{17}]$ gives an analysis of 22.61% C and 3.86% H; found: 22.44% C, 4.19% H.

(59) $[O_{1.5}SiCH_2CH_2SiO_{1.5}]_{10}[O_{1.5}SiC_8H_{17}]$ $[CN(C_6H_4)_2(CH_2)_7CH_3]_3$ gives a calculated analysis of 46.28% C, 5.63% H, and 1.78% N; found: 46.08% C, 6.14% H, and 2.22% N. This corresponds to 37 wt % 8CB.

(60) The pore volume filling was calculated using the pore volume determined from gas adsorption and an estimated density for 8CB of 1.0 g cm$^{-3}$.

(61) Guégan, R.; Morineau, D.; Lefort, R.; Béziel, W.; Guendouz, M.; Noirez, L.; Henschel, A.; Huber, P. *Eur. Phys. J. E* **2008**, *26*, 261−273.

(62) Wittebrood, M. M.; Luijendijk, D. H.; Stallinga, S.; Rasing, Th. *Phys. Rev. E* **1996**, *54*, 5232−5234.

(63) Ondris-Crawford, R. J.; Crawford, G. P.; Doane, J. W.; Žumer, S. *Phys. Rev. E* **1993**, *48*, 1998−2005.

(64) Iannacchione, G. S.; Finotello, D. *Phys. Rev. Lett.* **1992**, *69*, 2094−2097.

(65) Iannacchione, G. S.; Crawford, G. P.; Žumer, S.; Doane, J. W.; Finotello, D. *Phys. Rev. Lett.* **1993**, *71*, 2595−2598.

(66) Sardashti, M.; Maciel, G. E. *J. Phys. Chem.* **1988**, *92*, 4620−4632.

(67) Buffy, J. J.; McCormick, M. J.; Wi, S.; Waring, A.; Lehrer, R. I.; Hong, M. *Biochemistry* **2004**, *43*, 9800−9812.

(68) Levitt, M. H. *Concepts Magn. Reson.* **1996**, *8*, 77−103.

(69) Finotello, D.; Iannacchione, G. S.; Qian, S. Phase Transitions in Restricted Geometries. In *Liquid Crystals in Complex Geometries Formed by Polymer and Porous Networks*; Crawford, G. P., Žumer, S., Eds.; Taylor & Francis, London, 1996; pp 325−343.

(70) Bellini, T.; Clark, N. A.; Muzny, C. D.; Wu, L.; Garland, C. W.; Schaefer, D. W.; Oliver, B. J. *Phys. Rev. Lett.* **1992**, *69*, 788−791.